ZERO POWER CONTROLE IN THE SINGLE AXIS CONTROLLED MAGNETIC BEARING

Orlando Homen de Mello, orlando.hmello@gmail.com
Escola Politécnica of São Paulo University, Av. Prof. Mello Moraes, 2231, 05508-900, SP Brazil

Isaias da Silva, isaias.silva@unifesp.br
Federal University of São Paulo, R. Prof. Artur Riedel, 720, 09972-270, Diadema –SP, Brasil

Fernando Antonio Camargo, fernandoantonio.camargo@gmail.com

José Roberto Cardoso, jose.cardoso@poli.usp.br

Oswaldo Horikawa, ohorikaw@usp.br
Escola Politécnica of São Paulo University, Av. Prof. Mello Moraes, 2231, 05508-900, SP Brazil

Abstract. This work is part of the development of an implantable Ventricular Assist Device (VAD) in which the pump rotor is suspended by a magnetic bearing. The magnetic bearing here utilized presents active control only in the rotor axial direction. In other directions, the rotor is retained by the attraction force generated by permanent magnets. During the operation of the VAD, a drag force acts in the rotor due to the pumping effect, forcing the rotor axially toward the fluid entrance duct. To react this force, a current circulates in the bearing actuators, resulting in power consumption and heat generation. In order to minimize thise problems, this work studies the application of a control technique known as "Zero Power Control (ZPC)" in the magnetic bearing. By the ZPC, the axial reference position of the rotor is automatically changed so that the load is counterbalanced only by forces generated by permanent magnets. Previous works concerning ZPC are revised, a method to apply the ZPC to the magnetic bearing is developed and finally, by tests, the developed ZPC algorithm is evaluated.

Keywords*: Zero Power Control, Virtual Zero Power, Ventricular assistance device, Magnetic Bearing, Bearingless*

1. INTRODUCTION

The Escola Politécnica of São Paulo University (EPUSP) and the Institute Dante Pazzanese of Cardiology (IDPC) is conducting a joint project aiming the development of an implantable Ventricular Assist Device (VAD). Based on a VAD of external use, developed previously by the IDPC (Andrade *et al*, 1996), the new VAD will feature a magnetic bearing to suspend the rotor without any mechanical contact of the rotor and other VAD components. With respect to the new VAD, authors already reported results of preliminary studies (Horikawa *et al*, 2008). The magnetic bearing to be applied is of a type presented at Silva *et al*, 2000 in which, the active control is executed only in the axial direction of a rotor. In remaining directions, excepting the rotation, motions of the rotor are retained only by the attraction force generated by pairs of permanent magnets. In this work this bearing is referred as AMB-EPUSP. This bearing is elected mainly because of its simplicity in terms of mechanical configuration and in terms of control system: important factors to increase the reliability of the bearing.

Figure 1 shows one possible configuration for the VAD that combines the VAD-IDPC and the AMB-EPUSP. Two electromagnetic actuators with ferromagnetic core are placed at the upper and lower extremity of the rotor. At the top surface of the lower actuator, a coil is set so as to works as a probe of a non-contacting inductive gap sensor. At both extremities of the rotor, cylindrical rare earth (NiFeB) permanent magnets are fixed. The attraction forces between these magnets and the ferromagnetic core confine the rotor in a central position. Due to the symmetry, the rotor is free for rotating. However, since the force between the magnets and the cores are of attraction, in the axial direction, the rotor is unstable, requiring an active control by using the position sensor, a PD type controller and the actuators.

When operating, the rotor of the DAV is submitted to a hydrodynamic drug force in the axial direction. If only the PD control is applied, an additional current, compatible with the drug force, is furnished to the electromagnetic actuators so as to compensate the position error caused by the force. This implies in significant power consumption and a problem of heat dissipation, since the DAV is being developed for intracorporeal usage. To minimize these problems, this work proposes the application of a control technique known as Zero Power Control (ZPC) control. The next section presents details of the ZPC.

2. PRINCIPLE OF THE ZPC

The magnetic levitation (MAGLEV) principle applied to magnetic bearings opens possibilities for eliminating the friction in the moving parts in rotary or linear motion mechanisms. These result in reduction of energy loss, no necessity of lubrication and a operation in high speeds.

The magnetic force that is exerted in the rotor can be of attraction or repulsion, and generated by permanent magnets or electromagnets. The magnetic levitations by means of controlled hybrid magnetic circuit, also called Permanent Magnetic Control (PMC), is nowadays an important requirement for methods of power and energy saving strategies in MAGLEV systems (Youn *et al*, 2001). PMCs used in ZPC have as main characteristics the negative stiffness since they operates in the attraction mode, thus reducing problems of demagnetization (Campbell, 1994).

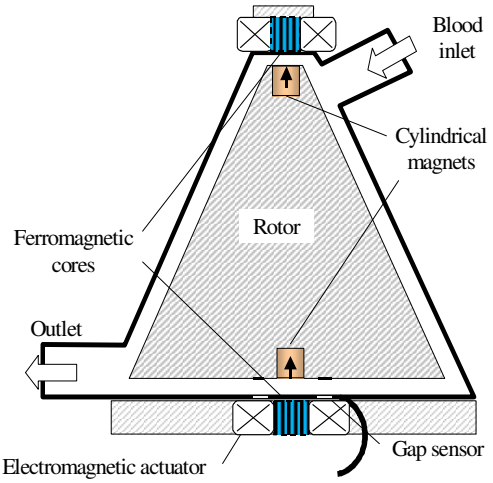

Figure 1. DAV-IDPC with EPUSP magnetic bearing

Figure 2 presents an example of MAGLEV of hybrid magnetic circuit. The example considers an electromagnetic actuator composed by a coil and a ferromagnetic core. Considering a cylindrical magnet as the object to be levitated, this will produces a magnetic attraction force (f_m) due to the influence of the ferromagnetic core in the actuator.

The distance between the actuator core and the object (magnet) in the Fig. 2, is referred as axial axis z, with the origin in the surface of the core. When in equilibrium, the relation among forces in the object is given as follows.

$$P = -(f_m + f_{em}) \tag{1}$$

Where, f_m is the magnetic force and f_{em}, the electromagnetic force, both actuating in the object.

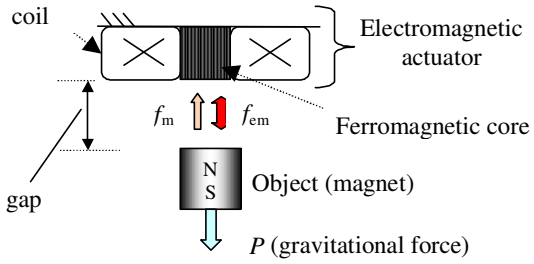

Figure 2. Example of hybrid MAGLEV system

The object shown in Fig.2 would be naturally suspended if the magnetic force (f_m) is equal to the weight (P). However a stable equilibrium by only permanent magnets is possible if the system is diamagnetic (Earnshaw, 1842). Thus a closed loop control system becomes necessary for achieving the equilibrium. The position control system operates applying an electric current to the coil of the actuator, necessary to generate an additional electromagnetic force capable of moving the object back to its reference position (z_{ref}).

Being z_{ZR} the axial position where f_m is equal to P, when the rotor is at z_{ZR}, the electromagnetic force is generated only when the control system has to correct the object position. This means that at z_{ZR}, the energy consumption necessary to levitate the object is minimized. Therefore, z_{ZR} is the position of so called zero power. However, this requires that the set point of the control system is equal to the z_{ZR}.

Figure 3 illustrates how the levitation with zero power can be executed manually. The user set the system so as to levitate the object keeping it in some position. Then, observing the current in the electromagnetic actuator, the user adjusts the voltage source (z_{ref}) until the current is minimum. The position thus obtained is the position z_{ZR} where the zero power is achieved.

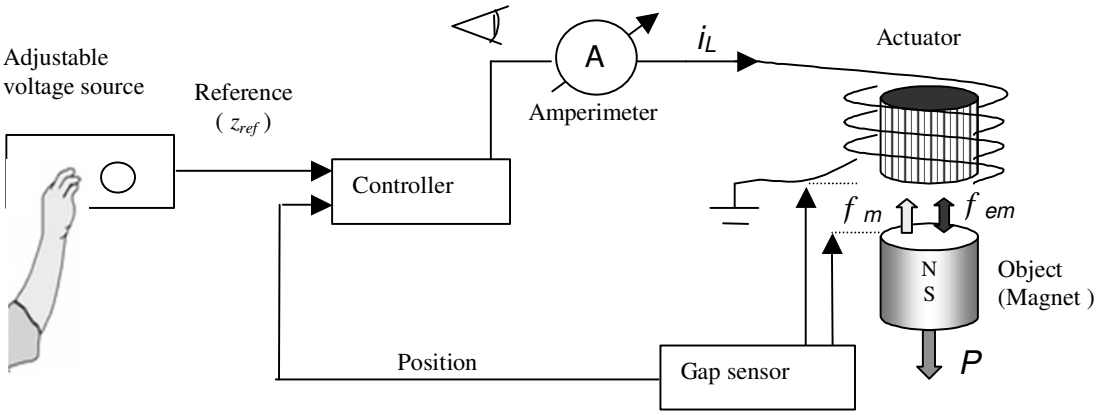

Figure 3. Manual zero power control in a MAGLEV system

There are considerable amount of works concerning the ZPC. The first work concerning this control technique is presented at Morishita, 1986, that aimed the minimization of the power consumption in a clean room transportation system based on MAGLEV. After this work, several applications are presented, for example: MAGLEV vehicles (Simpson, 1976), vibration insulation (zero compliance) (Mizuno, 2002) and axial type VAD (Paden, 2002).

Based on above described principle of ZPC, the aim of this work is to develop a control algorithm that automatically determine the natural equilibrium position (z_{ZR}) of a hybrid magnetic bearing with active control in a single direction, the AMB-EPUSP, that is presented in more details in a forward section.

3. THE AMB-EPUSP AND THE ZPC

Although the AMB-EPUSP presented at Silva, 2000 differs from that presented in Fig.1, the working principle is the same. In Fig.1, a rotor has magnets polarized in the axial direction, fixed to each extremity. Facing each magnet, an electromagnetic actuator composed of a coil and a ferromagnetic core is fixed to the VAD body. A gap of few millimeters is set between each magnetic pair composed by the magnet and ferromagnetic core. The attraction force between the elements of the magnetic pair, a positive stiffness is generated in the radial directions, thus the rotor is confined in the central position. Due to the bearing symmetry, the rotor is free for rotating. However, since the forces between magnetic pairs are of attraction, the stiffness in the axial direction is negative. This means that the rotor is unstable in terms of axial position and an active control of the rotor axial position becomes necessary. Thus, a non-contact inductive type sensor is installed to measure the rotor axial position, the sensor reading is sent to a Proportional Derivative (PD) type controller and the controller send a command signal to the electromagnetic actuators through power amplifier.

Figure 4 presents the block diagram of the AMB-EPUSP and the Table 1, the list of symbols used in Fig.4.

Based on the principle described in previous section, a ZPC algorithm is developed. The ZPC is based on the monitoring of the current in the actuator. As shown in Fig.4, the transfer function G_1 that represents the dynamics of the power amplifier and the electromagnetic actuator, is of first order. Moreover, the natural frequency of the rotor (around 62 rad/s) is much time lower than that of the electromagnetic actuator (Krad/s order). These facts, associated with the assumption that the ZPC considers only static or quasi-static loads applied on the rotor, make possible the following simplification: the current (I) in the actuator is considered proportional to the voltage (V) applied to the actuator. Thus, instead measuring the current, a more accessible internal variable V_c, the controller output, is measured. This procedure avoids the use, for example, of a shunt circuit to measure the current, simplifying the control system hardware.

Figure 5 shows the AMB-EPUSP block diagram with the block corresponding to the ZPC. Following the idea of the ZPC executed manually, the element responsible for the ZPC is inserted in the AMB system so as to change the reference position according to the current in the actuator.

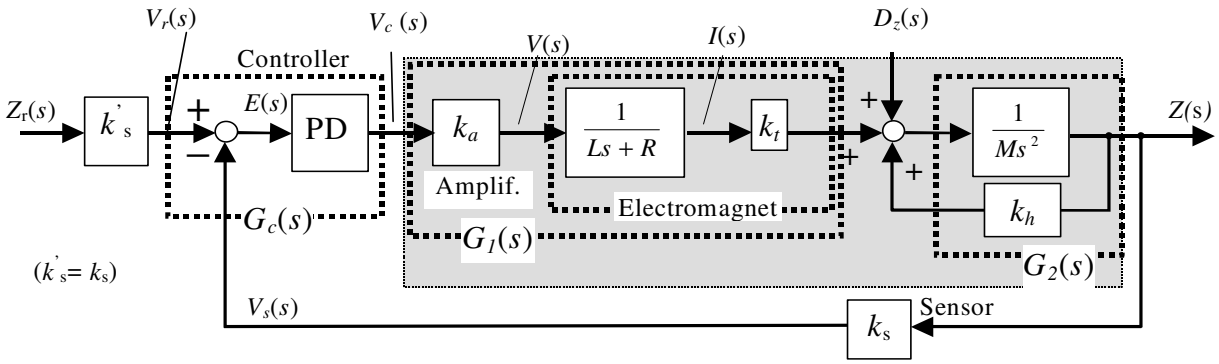

Figure 4. Block diagram of the AMB EPUSP control system (Silva,2000).

Table 1 List of symbols used in Fig.4

Symbol	Meaning	Unit
Z	Axial position of the rotor	Meter
Z_r	Reference position	Meter
V_r	Reference voltage	Volt
E	error	Volt
V	Amplifier output	Volt
L	Coil inductance	Henry
R	Coil resistance	Ohm
I	Current in the coil	Ampere

Symbol	Meaning	Unit
D	Disturbance force	Newton
M	Mass of the rotor	Kilogram
V_c	Controller output	Volt
V_s	Sensor output	Volt
k_t	Electromagnetic constant	Newton / Gauss
k_h	Magnetic constant	Newton / Gauss
k_a	Power amplifier gain	Volt / Volt
k_s	Sensor gain	Volt / Meter

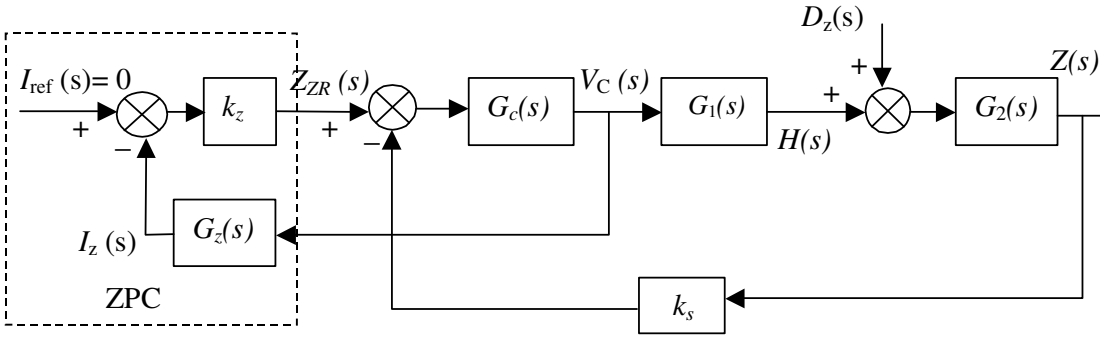

Figure 5. Block diagram of the AMB-EPUSP with the ZPC.

Figure 6 presents details of the block that executes the ZPC. In the figure, block (1) is responsible for calculating the average current to the actuator (I_{LM}). The calculation of the average current is equivalent to the use of a low pass filter that is essential to avoid derivative feedback in the control. Block (1) operates according to the following equation.

$$I_{LM}(t) = V_m k_a \frac{(1 - e^{-t/\tau})}{R} \tag{2}$$

Where k_a is the gain of the power amplifier that supply current to the actuator, τ is the time constant of the electromagnetic actuator, R is the resistance of the electromagnetic actuator, $t \approx t_{am}$ is the sampling time used in the digital control and V_m is the average voltage applied to the actuator given by:

$$V_{m,n} = \frac{(V_{c,n} + V_{c,n-1})}{2} \tag{3}$$

Here, $V_{c,n}$ is the actual output voltage of the controller and $V_{c,n-1}$, output voltage in the previous sampling period.

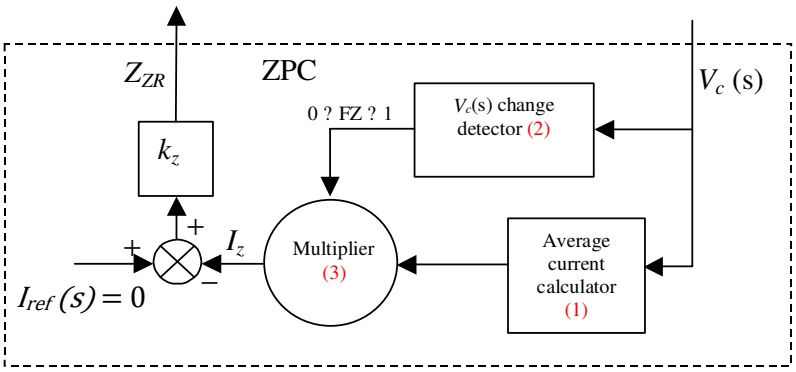

Figure 6. Block diagram of the ZPC

The block (2) in the Fig.6 determines a factor F_z that represents the strategy that, for fast disturbances the control action is taken by the PD controller. The ZPC works when variation in the disturbance is enough low. This scaling factor is inversely proportional to the variation ratio of the control voltage V_c. It is zero for a maximum variation and 1 when the voltage does not changes. F_z is calculated as follows.

$$F_z = \frac{10 - \left| \frac{V_{c,n} - V_{c,n-2}}{2} \right|}{10} \qquad (4)$$

Block (3) in the Fig.6 determines the term I_z that represents the steady state current in the ZPC, given by:

$$I_z = I_{LM} \cdot F_z \qquad (5)$$

Considering that I_z is proportional to the error between the previous reference position (Z_{ZR}) and the future natural equilibrium point (Z'_{ZR}) following is obtained:

$$Z_{ZR} = Z'_{ZR} = I_z k_z \qquad (6)$$

Where k_z is the gain of the ZPC.

The main function of above described blocks is to collect the voltage signal obtained from the PD controller output, convert the voltage to current and filter out harmonics of higher order. To filtering the signal an algorithm is developed intuitively. Experiments presented in next sections, show its efficiency.

4. EXPERIMENTS AND RESULTS

Figure 7 shows schematics of the prototype AMB-EPUSP used in tests. The bearing is digitally controlled by using IBM-PC standard computer, a A/D board of 16 bits resolution and 100 KHz sampling rate also equipped with a D/A channel of 16bit. The power amplifier is of linear type with a nominal capacity of 3 amperes current; 12V supply voltage and voltage gain of 10.

Figure 8 presents detailed schematics of the bearing and the picture of the bearing. A conical shaped rotor simulates its application to the VAD-IDPC. Fig.9 presents picture of the experimental VAD.

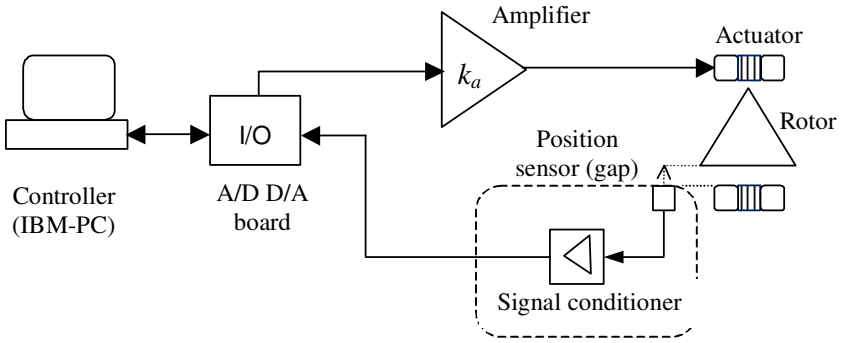

Figure 7. Schematics of the AMB EPUSP used in the tests

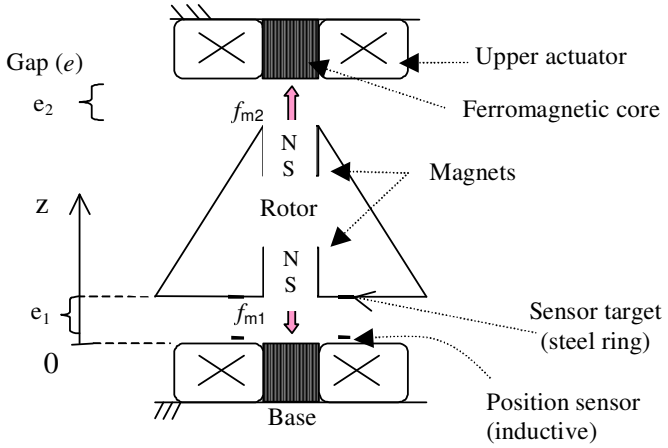

Figure 8 Configuration of the experimental AMB and magnetic forces .

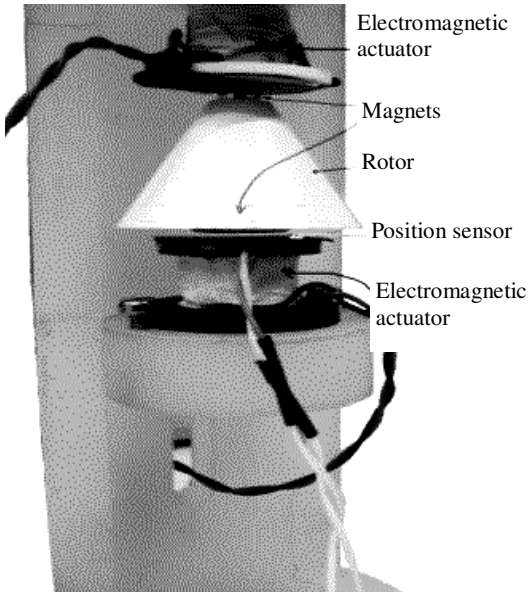

Figure 9. The experimental AMB.

4.1. Magnetic end electromagnetic forces in the AMB

Figure 10 presents results of numerical simulation by Finite Element Method (FEM) of the force exerted by the electromagnetic actuator on the rotor, for different values of gaps and current. This graph is for one pair composed by a magnet and an actuator. The curve obtained when the current is null, corresponds to the force generated only by the permanent magnet. One can observe that the force decays drastically as the gap increases, becoming insignificant for gaps larger than 4mm. By reverting the sense of the current in the actuator, a component of repulsion is summed to the attraction force generates by the magnet. However, the force between the actuator and the magnet fixed to the rotor is of attraction almost in all situations.

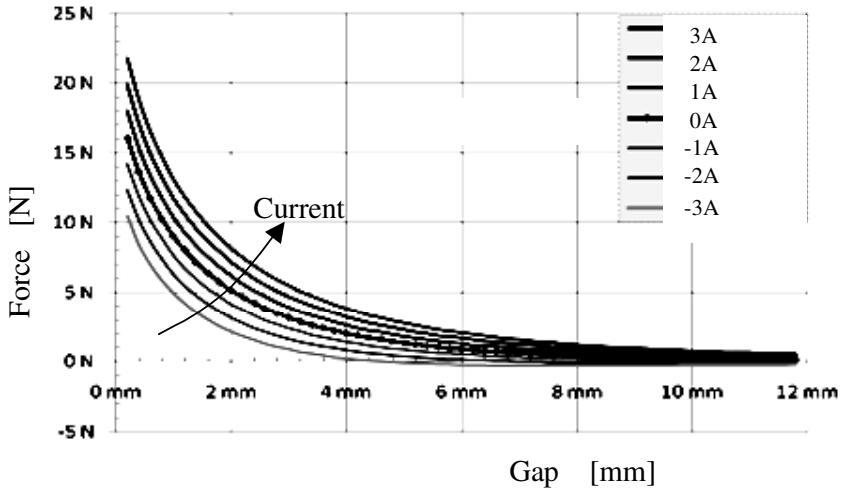

Figure 10. Relationship between force and gap

Figure 11 presents numerical simulations by FEM of forces, now considering the two magnetic pairs, one at each extremity of the rotor. The region between 1.3 mm to 2.7 mm of gap indicates the operating region of the AMB. The operation in this region assures that the gap is small than the limit of 4mm, as mentioned above with respect to the Fig.10. Also, the operation of the AMB in the mentioned region assures good linearity of the force versus gap relation.

As mentioned before, the ZPC changes the set point of the AMB in a position where the load applied to the rotor is counterbalanced by magnetic forces. However, this change in the set point must be within the mentioned limits. Otherwise, the electromagnetic actuators will not be able to exert control action in a stable way.

4.2. Stepwise load response

An oscilloscope samples the readings of the axial position sensor when a load is applied manually. Although manual, the load is applied so that a minimum amount of impact is applied to the rotor.

Figure 12(a) presents the response in terms of current as function of the stepwise disturbance load without the ZPC. In the steady state condition, besides a small deviation in the rotor position, it is possible to observe a constant current circulating in the actuator.

Figure 12(b) presents the same response with the ZPC turned on. A transitory current is observed for a moment, but rapidly, the position of the rotor is changed and the average current converges to zero.

Above results confirm the efficiency of the developed ZPC algorithm.

4.3. Ramp wise load response

Figures 13(a) and 13(b) shows the current in the actuator when a ramp load is applied to the AMB, with and without the ZPC, respectively. These results show that the developed ZPC algorithm is efficient not only to static loads but also for dynamic loads with low harmonic frequency components. The next item describes some comments with this respect.

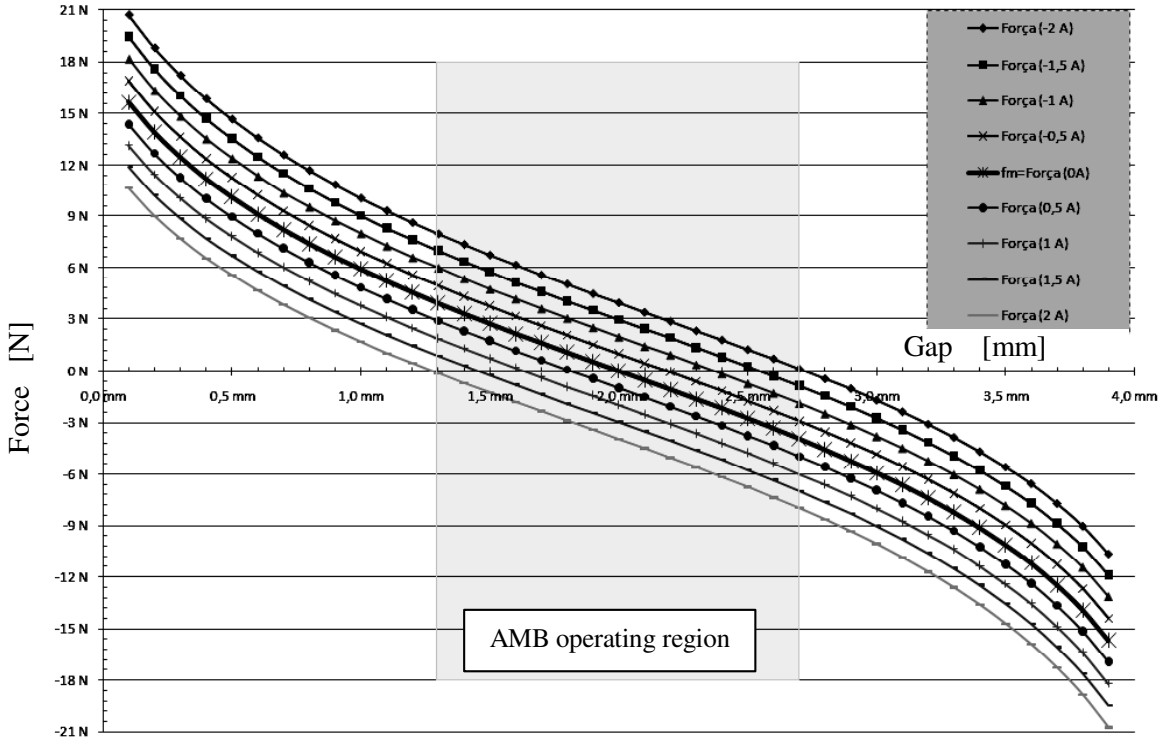

Figure 11. Force vs gap relation in the complete AMB

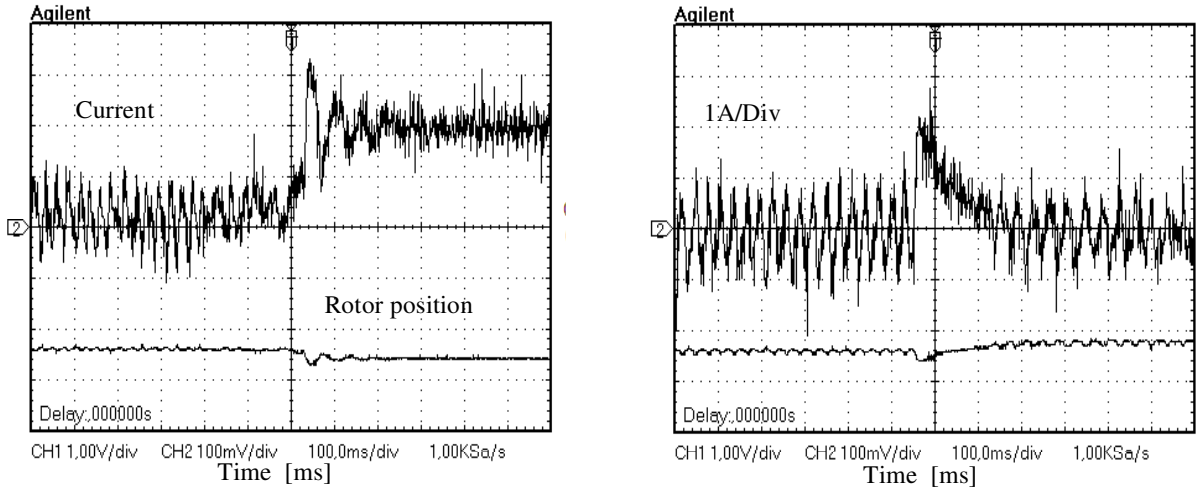

(a) Without ZPC (b) With ZPC

Figure 12. Response in current to stepwise load

4.4. Limits of the AMB

Figures 14(a) and (b) shows result of a test where a ramp wise load is applied to the rotor until the control breaks down. Although these tests are executed in similar manner of the previous tests, in this case, larger loads are considered and the apparatus used to apply the loads was not capable of increasing the load linearly. The Figures 14 (a) and (b) show respectively the case without and with the ZPC. In both results, it is possible to observe that when the load applied to the rotor reaches some value, the active control stops to work and the rotor suddenly moves to another position, and

stops when touches the actuator. This occurs because the load exceeds the maximum force that electromagnetic actuators are capable to exert on the rotor. However, when the ZPC is used, Fig.14(b), the AMB resists to a load clearly larger than that observed in Fig 14(a), without ZPC. An increase of about 20% is observed. It is important to notice that in these experiments, the rotor eventually reaches axial positions outside the limits showed in Fig.11. Thus, the effects of non-linearity become prominent. When the load is applied, the ZPC conducts the rotor until a position where the axial stiffness due to magnetic forces is higher: the left and right extremes of the graph shown in Fig.11. This increase in the stiffness probably promotes the increase in the load capacity by the ZPC. This fact may be interesting in AMB applications, however a problem must be solved. It is reasonable to suppose that when starting up an AMB, the rotor is contacting one of the actuators. If the gap is set outside the limits of the actuators, the AMB will not be able to start.

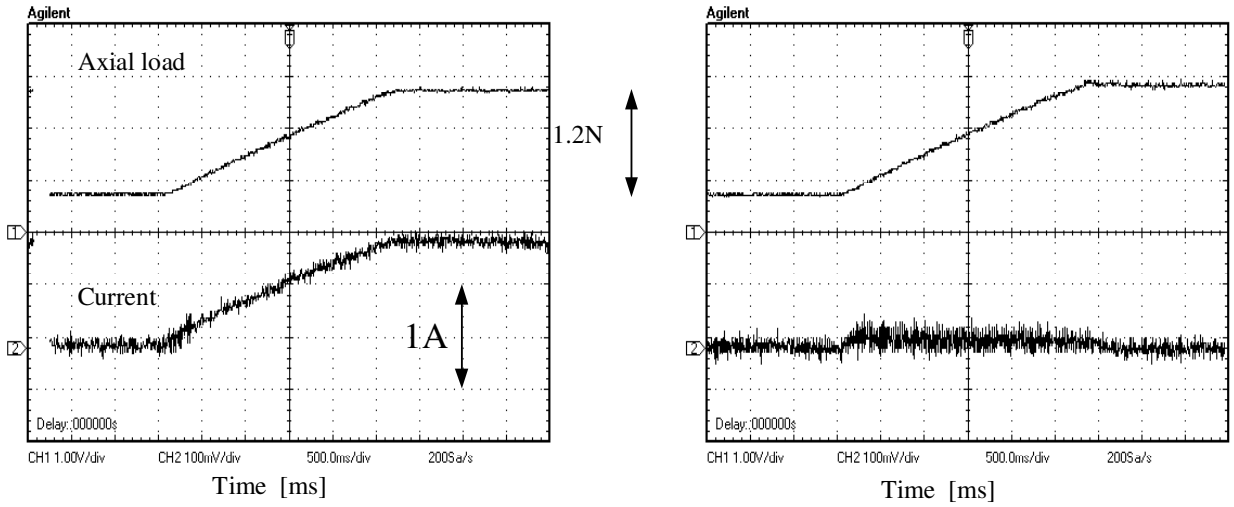

(a) Without ZPC (b) With ZPC

Figure 13. Response in current to ramp wise load

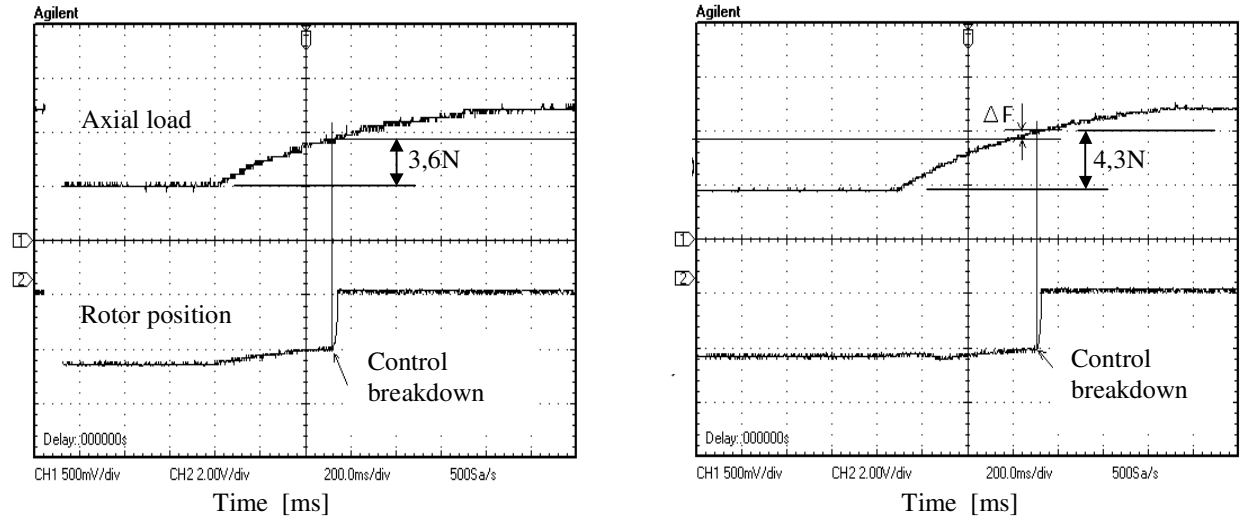

(a) Without ZPC (b) With ZPC

Figure 14 Response in position to a ramp wise load until the control breakdown

5. CONCLUSIONS

According to principles presented by other authors, a strategy to implement the Zero Power Control, ZPC, is developed to be applied in the AMB-EPUSP. The AMB-EPUSP will support the rotor of blood pump for intracorporeal use (VAD-IDPC). When the VAD is operating, the rotor is submitted to a hydrodynamic drag force, making the AMB consume significant current and generating heat. The ZPC is essential to minimize these problems.

An algorithm to execute the ZPC in the AMB EPUSP is developed and tests demonstrated its efficiency.

In this work, the frequency domain where the ZPC works was determined experimentally. Although it was demonstrated that the developed strategy is efficient also for dynamic loads, it is necessary to define a method to determine the limit frequency for the ZPC effect. The effects of the ZPC conflicts with the effects of the PD controller that is the basic controller of the AMB. This will require a more rigorous modeling of the AMB with the ZPC element, analyzing its stability. This will constitute future themes for this work.

6. ACKNOWLEDGEMENTS

This work received finantial suppports from Fundação de Amparo à Pesquisa do Estado de São Paulo, FAPESP (Brazil), process number 2006/58773-1.

7. REFERENCES

Andrade, A., Biscegli, J., Dinkhuysen, J., Sousa, J.E., Ohashi, Y., Hemmings, S., Glueck, J., Kawahito, K. and Nose, Y., 1996, Characteristics of a Blood Pump Combining the Centrifugal and Axial Pumping Principles: The Spiral Pump, Artificial Organs, Vol.20(6), pp.605-612.

Campbell, P., 1994, “Permanent Magnet Materials and Their Application”, Vol.I, Cambridge University Press, 191 p..

Earnshaw, S., 1842, "On the Nature of the Molecular Forces which Regulate the Constitution of the Luminiferous Ether". Trans. Camb. Phil. Soc., 7, pp.97–112.

Horikawa, O., Andrade, A.J.P, Silva, I. and Bock, E.G.P., 2008, Magnetic Suspension of the Rotor of a Ventricular Assist Device of Mixed Flow Type. Artificial Organs, Vol.32(4), pp.334-341.

Mizuno, T., 2002, “Vibration isolation system using zero-power magnetic suspension”, Preprints of 15th World Congress IFAC, p.955.

Morishita M. and Azukizawa T., 1988, “Zero power control method for electromagnetic levitation system”, Trans IEE Japan;108-D, pp.447–454.

Paden, B., 2002, “The Streamliner Artificial Heart”, Proc. of the XIV Brazilian Automatic Control Conference, Natal, Brazil, sept 2002.

Silva, I. and Horikawa, O.. 2000, “An 1-DOF Controlled Attraction Type Magnetic Bearing”, IEEE Trans. on Industry Applications, Vol.36 (4), p.1138.

Simpson, P. A., 1976, “Virtually Zero Power Linear Magnétic Bearing”, US Patent 3,937,148. Feb 1976

Youn H. Kim, Kwang M. Kim, Ju. Lee, 2001, “Zero Power Control with Load Observer in Controlled-PM Levitation”, Trans. IEEE Korea, Vol. 37, No.4.

8. RESPONSIBILITY NOTICE

The authors are the only responsible for the printed material included in this paper.